

Studying the spontaneous polarization and dielectric response of La: BiFeO₃ nanocrystal (NCs)

Rezq Naji Aljawfi^{1,*}, Hashim Al-Sanaa¹ & Shalendera Kumer²

¹Department of Physics, Ibb University, Ibb, 70270, Yemen

¹Department of Physics, College of Sciences, King Faisal University, Al-Asha31982, Saudi Arabia

*Corresponding Authors: E. mail: rizqnaji@yahoo.com

DOI: <https://doi.org/10.56807/buj.v2i2.45>

Abstract

We studied the dielectric response and ferroelectric ordering of BiFeO₃ and La doped bismuth ferrite (Bi_{0.97}La_{0.03}FeO₃) nanocrystal (NCs) synthesized through sol-gel conventional route. XRD refinement revealed the formation of rhombohedral distorted perovskite structure with negligible secondary phase. The frequency dependent dielectric constant $\epsilon(\omega)$ showed a rapid decrease in the dielectric at low frequency (1 MHz), and become almost constant at high frequency. The surface charge and orientation polarizations are likely to be predominant governing the dielectric response. The ferroelectric measurements (P-E curve) displayed remnant polarization, which were about 0.60 $\mu\text{C}/\text{cm}^2$ at 17.35 kV/cm for Bi_{0.97}La_xFeO_{0.03}. Our study confirmed a weak offset in the crystal structure, dielectric response and ferroelectric properties of BiFeO₃ NCs as a function of La dopant ion.

Keywords: BiFeO₃, XRD, Dielectric properties, Ferroelectric loop.

دراسة الاستقطاب التلقائي والاستجابة العازلة للكهرباء La: BiFeO₃ nanocrystal (NCs) الملخص

لقد درسنا الاستجابة العازلة والترتيب الكهروحراري لـ BiFeO₃ و La doped bismuth ferrite (Bi_{0.97}La_{0.03}FeO₃) بلورة نانوية (NCs) تم تصنيعها من خلال طريق sol-gel التقليدي. يوضح XRD تكوين بنية perovskite مشوهة معينة الشكل مع طور ثانوي مهم. أظهر ثابت العزل المعتمد على التردد $\epsilon(\omega)$ انخفاضاً سريعاً في العازل عند التردد المنخفض (1 ميجاهرتز)، وأصبح ثابتاً تقريباً عند التردد العالي. من المرجح أن تكون استقطابات شحنة السطح والتوجيه هي السائدة التي تحكم استجابة العزل الكهربائي. أظهرت القياسات الفيروكهربائية (منحنى P-E) استقطاباً دائماً، والذي كان حوالي 0.60 $\mu\text{C}/\text{cm}^2$ عند 17.35 كيلو فولت / سم. أكدت دراستنا وجود إزاحة ضعيفة في التركيب البلوري، والاستجابة العازلة، والخصائص الفيروكهربائية لـ BiFeO₃ NC كدالة لأيون La dopant.

1. Introduction

The multiferroic is a class of materials having simultaneously ferroelectric and ferromagnetic orderings. The bismuth iron ferrite (BiFeO₃) based multiferroic, with fascinating physics properties, have drawn a great attention due to its potential applications in spintronics, sensors, data storage microelectronics and actuators. Where, BiFeO₃ perovskite system has a rhombohedral R3c crystallographic structure (Fiebig, 2005, 38). In a

spontaneous polarization, 6s² configuration of Bi³⁺ ion inserts center deformation resulting in BiFeO₃, whereas the extremely change interactions in between Fe³⁺ ions calculated magnetic ranging in these materials (Hill, 2000, 6694). In addition, it was large curie temperature ($T_C \sim 1102$ K) and G-type antiferromagnetic Neel temperature ($T_N \sim 644$ K) (Chaudhuri, 2012, 1057. Chen, 2012, 108). For rejecting the secondary peak on a morphological shift and amending ferroelectric and ferromagnetic

properties of those materials, it was observed that partial substitution of rare-earth metal ions at A-site of BiFeO_3 can be manufactured (Lazenka, 2012, 123916. Yuan, 2006, 052905. Duan, 2001, 259). Moreover, some difficulties connected with BFO_3 (Ahmed, 2013, 23). It was a minimum melting and maximum explosive point. Therefore, it becomes hard to synthesize pure BiFeO_3 pattern as both deficiency and excess of BFO leads to bismuth rich and deficient patterns (Ahmed, 2012, 4470). Lots of confounding reports are presented in survey of literature related to temperature and pattern conversions in BiFeO_3 (Casper, 2013, 1578). Valency variations in iron between iron two positive and iron three positive ions cause a maximum leakage current. Minor secondary peaks of bismuth rich and bismuth inferior patterns are known not to impact them electric and structural properties but even small impurity level was a tremendous impact of optical, electrical and dielectric materials. Looking to the technological importance and quest for revealing the substitutional effect at A (Bi)-site. We have prepared BiFeO_3 and $\text{Bi}_{0.97}\text{La}_{0.03}\text{FeO}_3$ by sol-gel and report the structural, dielectric and ferroelectric properties. The effect of defect on the dielectric response and spontaneous polarization have been investigated. Our study showed that the BiFeO_3 system seems relatively high stable, where, the substitution of La dopant ions affect slightly on the local structure, lattice parameters, dielectric response and ferroelectric properties.

2. Experimental details

Our nanostructured BiFeO_3 and $\text{Bi}_{0.97}\text{La}_{0.03}\text{FeO}_3$ were synthesized by using sol-gel simple route. In which, the bismuth nitrate pentahydrate $[\text{Bi}(\text{NO}_3)_3 \cdot 5\text{H}_2\text{O}]$, and iron nitrate nonahydrate $[\text{Fe}(\text{NO}_3)_3 \cdot 9\text{H}_2\text{O}]$, were used as precursors and weighed properly to make a solution of 0.1M. For synthesis of La doped BiFeO_3 , following procedure

has been used: The double distilled water and citric acid ($\text{C}_6\text{H}_8\text{O}_7$) were taken in a beaker and stirred to make a solution. This solution was used as solvent. The ratio of metal nitrate and citric acid was kept 1:1. Afterwards, bismuth nitrate pentahydrate was added to the solvent and some amount of concentrated nitric acid (HNO_3) was used to dissolve bismuth ferrite. Later on, lanthanum nitrate $[\text{La}(\text{NO}_3)_3 \cdot x\text{H}_2\text{O}]$ and $[\text{Fe}(\text{NO}_3)_3 \cdot 9\text{H}_2\text{O}]$ was added to the above solvent. Finally, ethylene glycol was added to the mixture and stirred at 90°C for the formation of gel. Then light orange-colored solution was obtained under vigorous stirring. The obtained powders were calcinated at 600°C for 2 hours to found La doped BFO ferrite nanocrystals. Then calcinated powders were taken into the required shapes by using die-press technique, in which, the calcined powder was filled into circular die with a diameter of 1 cm and pressed using hydraulic pressure of 1 ton. The thickness of the pellets was maintained ~1 to 1.5 mm. The both parts of the pallets have been polished with silver paste because it acts electrode, contact for calculating the dielectric materials. After the complete chemical synthesis and heat treatment of the synthesized products, the samples were characterized using XRD, dielectric measurements, PE-loop measurement and UV-vis absorption spectroscopy. The XRD in the range of $20-70^\circ$, with Cu $K\alpha$ radiation ($\lambda = 0.154178 \text{ nm}$) was used to find the crystallographic structure. And the frequency range from 1 to 5 MHz. P-E loop has been traced using P-E Loop Tracer with an internal capacitance of 100 nf and internal resistor of 1M at Triangular wave. The maximum field of 5 KV/cm was used in MARINE PE – 01 PE Loop Tracer System.

3. RESULTS AND DISCUSSION

3.1. XRD analysis

The crystal structure of BiFeO_3 and $\text{Bi}_{0.97}\text{La}_{0.03}\text{FeO}_3$ NCs have been studied via XRD technique. The XRD data have been analyzed precisely by using

Rietveld refinement code implemented in FullProof open access software program.

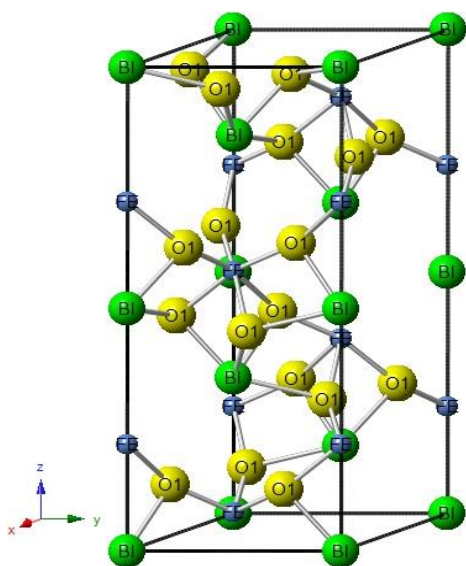


Fig.1 (a) the unit cell representation based on CIF file
Table1: The remnant polarization and coercive electric fields for La concentration.

La Content (%)	Remnant Polarization ($\mu\text{C}/\text{cm}^2$)	Coercive Electric Field (kV/cm)
0%	0.15	-6.5
3%	0.60	-10

Fig. 1 (b) shows the XRD profile of the studied samples, where the small black dots represent the experimental XRD spectra, the fine red lines stand for the fitting curves with 0.28-1.15 goodness factors (χ^2). The difference between the measured and fit patterns can be seen in the pink line and the exact location of Bragg angles are depicted by the blue vertical lines. The well matching between the experimental and calculated diffraction peak reveals that all the samples of La doped BFO_3 are crystalized in rhombohedral distorted perovskite structure with $R3c$ space group. The weak extra peak at $2\theta = 28^\circ$ may be originated to presence of a negligible secondary phase of $\text{Bi}_2\text{Fe}_4\text{O}_9$ according to

JCPDS card No. 01-074-1098. The obtained crystallography information file (CIF) have been employed to simulate the unit cell geometrical structure as seen in Fig. 1 (a). From which, the Bi ions are located at corner of cubic (A site), Fe ions at the center of the octahedron (B site) and contribute. Fe/La ions are coordinated by six ligands of oxygen atom.

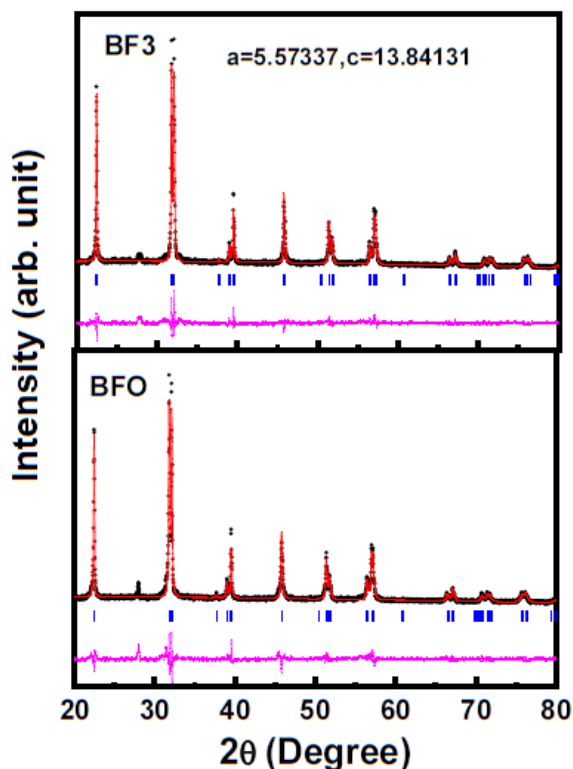


Fig. 1: (b) XRD profile of BiFeO_3 and La doped sample,.

The La dopant ions are expected to occupy the A sites of Bi ions or B sites of Fe ions, which cause an offset in the local environment around the La ions by changing the angles and chemical bond length in the short-range structure. Hence, the lattice parameters of pure BFO_3 ($a=5.57392$, $c=13.8454$) decreases with La doping increase to be $a=5.57337$, $c=13.8413$ for the 3 % doped BFO_3 NCs. Debye-Scherrer equation suggested a slight decrease in the crystallite sizes (D) and found to be 59 nm and 57

nm for pure BFO and 3 % La doping in BFO₃ NCs respectively.

3.2. Dielectric response

The relative permittivity (ϵ) can be expressed as $\epsilon = \epsilon' - i\epsilon''$, where ϵ' is the real part of dielectric constant, which describes the stored energy per cycle accompanied with the polarizations, and ϵ'' is the complex part of ϵ , which reflects the energy loss per cycle, due to conductivity. Fig. 2 (a) and (b). depicts the typical frequency dependent dielectric response for pure BiFeO₃ and La (3 % and 5 %) doped BFO₃ NCs. It can be noticed clearly that, the dielectric constant ϵ' and ϵ'' at low frequency (1MHz) is high and their values were found to be 67, 152 and 135 for pure BFO₃ and BFO₃ doped with 3 % and 5 % La dopant ions respectively. The values of dielectric constant decreases rapidly as the frequency increases and becomes saturated and almost constant at high frequency (5 MHz).

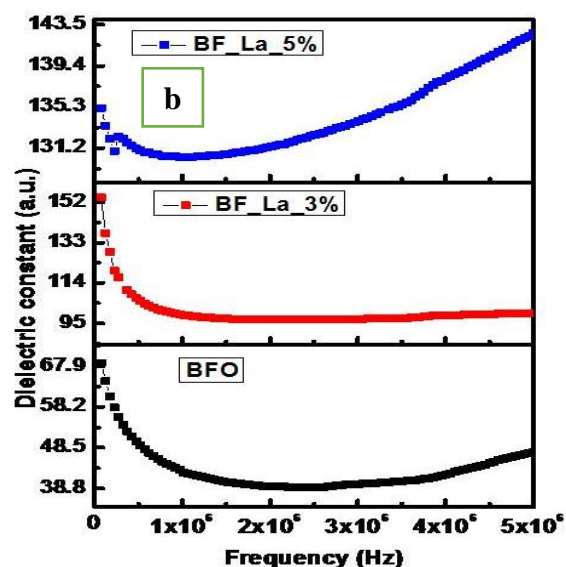
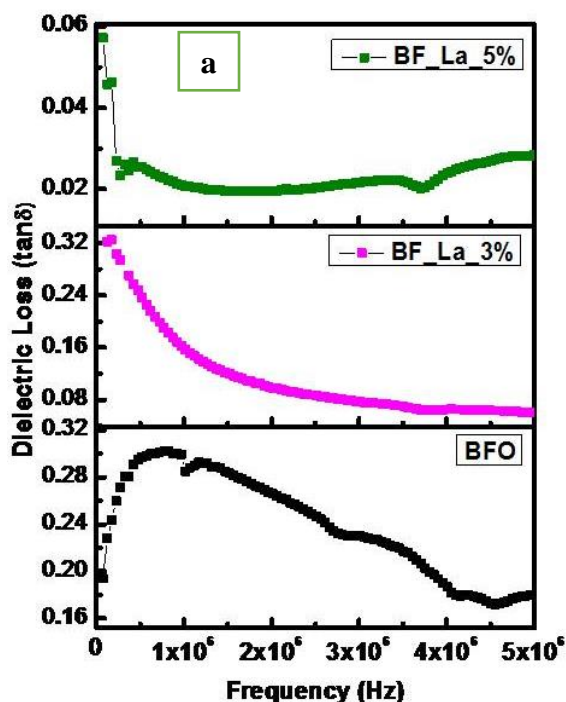


Figure 2(a): Frequency dependence of dielectric constant of $\text{Bi}_{1-x}\text{La}_x\text{FeO}_3$; and (b) Variation of dielectric loss as a function of frequency

This behavior tendency is familiar in nanostructured dielectric and semiconductor composites. Where at low frequency, the interfacial/space charge possess the capability to be aligned and oscillated under the effect of external alternative electric field, which means high interfacial polarization and then high dielectric constant. With progress increase in the frequency, the charge space cannot follow the external frequency. which leads to decrease the polarization and the associated dielectric response up to 0.5 MHz. Above 0.5 MHz the dielectric becomes almost constant. In general, the long relaxation time (τ) of the polarization with respect to the frequency of electric field causes a reduction in the dielectric constants. All polarization such as electric, ionic, dipole all are expected to contribute in the dielectric response. However, the space charge and ionic/orientation polarization are more significant in case of BiFeO₃. Where, the dislocated atoms such as Vo at the surfaces and interfaces, as detected in PL spectra, leaves two electrons behind, one is predicted to be captured by Fe³⁺ ions reducing their valence state (Fe³⁺) to be Fe²⁺. and the

other electron contributes in the space charge with weak energy (donor band). Thereby, the dielectric response is related to space charge polarization (surface) based on Maxwell–Wagner interfacial model (Maxwell, 1873, 328) (Prodromakis, 2009, 6989) and Koop's phenomenological theory (Koop, 1951, 121). In accordance with this model, the dielectric or semiconductor medium is made up of dielectric or semiconducting grains that are separated by insulating grain boundaries. Under the effect of alternative external electric field, the charge carriers can move inside the grains freely but at the grain boundaries the positive and negative charge carriers would be accumulated at the opposite site of NCs surfaces, consequences a large polarization and high dielectric constant. The small conductivity of surfaces contributes to the high value of dielectric constant at low frequency. Furthermore, the surface defects like dangling bonds, oxygen vacancy (VO) and micro-pores at the surfaces of NCs leads to a change in the positive and negative space charge distribution at the interfaces. It is well known that in case of NCs, the surface has a great significant owing to high surface to volume ratio and increase the surface defect like Ov. Hence, the O loss in the O ligand around the B site (Fe or La substituted). It predicted that the substitution of La ion in the lattice site of Fe induces further Vo increasing the charge space and polarization and dielectric that is may be the reason behind the observed increase in the dielectric constant at high frequency. The interfaces were found to be more effective at lower frequencies while the semiconductor core are more effective at higher frequencies. The increasing in the dielectric curve at high frequency region with increasing La dopant concentration may be due to the electronegative of La (1.1) lower than that of Fe (1.83) that makes the ionic bonds of $\text{La}^{2+} - \text{O}^{2-}$ weaker than that of $\text{Fe}^{2+} - \text{O}^{2-}$ bonds consequences an increase in ionic polarization and dielectric constant

at high frequency as seen in the end of spectral line of .5% doped BFO_3 NCs.

In BFO_3 rhomboidal crystal structure the B center at Fe^{3+} sites does not lie in the center of octahedron exactly but it is shifted down which causes an orientation spontaneous polarization that contribute significantly on the dielectric constant and the ferroelectric properties (P-E) hysteresis loop as seen in next section.

3.3. P-E polarizability

Fig. 3 (a) and (b) show the polarization versus applied electric field (P-E) for pure BFO_3 and La

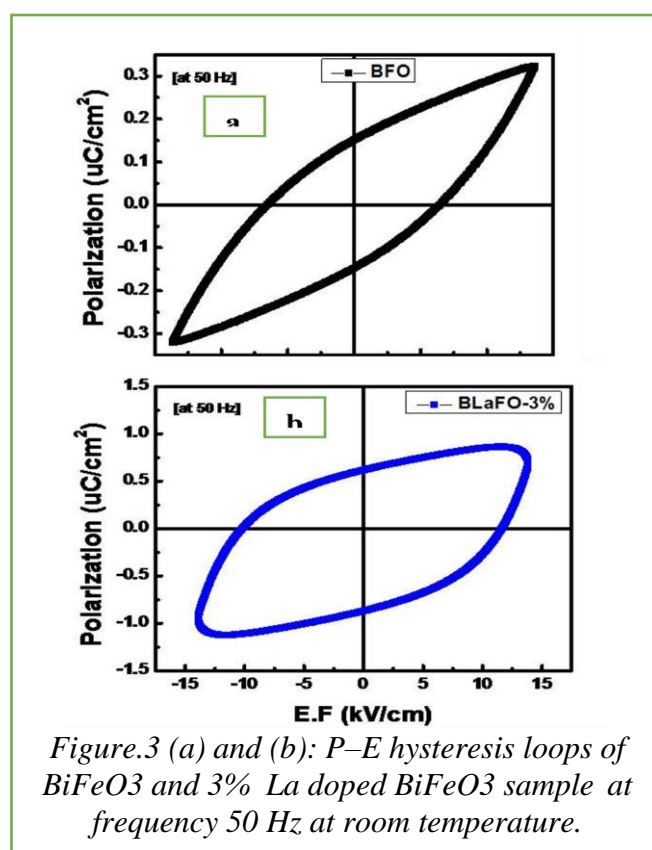


Figure.3 (a) and (b): P–E hysteresis loops of BiFeO_3 and 3% La doped BiFeO_3 sample at frequency 50 Hz at room temperature.

3% doping in BFO_3 samples at low frequency of 50 Hz at room temperature. With the increase of applied electric field, the polarization increased and showed saturation.

The remnant polarization shows decreasing with the increase of La dopant concentration, in contrast with the coercivity, which exhibit an increase in sequence with increasing the La content, all values are summarized in table 1. The applied electric field acts on the charge of inversion of ferroelectric domains, which leads to P-E hysteresis loop, and the variation in the parameters of P-E curve is related to different concentration of free electron charges in the core of NCs and charge traps at the surfaces and interface. The comparatively high conductivity of BiFeO₃ is known to be attributed to the redox cycle of Fe³⁺/Fe²⁺, near oxygen vacancies for charge recommendation. For high conductivity, the presence of Fe²⁺ ions and oxygen deficiency lead it. In the dramatically change a La substitution is striking that only electric polarization behavior, although the remnant polarization is still far less than the expected value of BiFeO₃ samples (0.82 μC/cm²) as predicted in Bi excess BFO series synthesized and analyzed in the present work.

4. Conclusions

BiFeO₃ and Bi_{0.97}La_{0.03}FeO₃ nanocrystals have been synthesized via sol-gel method. The XRD patterns obtained the single crystalline pattern nature with rhombohedrally distorted perovskite structure of nanocrystals for La doped BFO samples and showed minor secondary peak (Bi₂Fe₄O₉) at 2θ = 28°. The crystal particle size has been observed 53-47 nm range for La doped samples. The dispersion nature of the dielectric material for La doped BiFeO₃ as a frequency of function was found according to interfacial polarization as predicted by the Maxwell-Wagner and Koop's theory. Polarization versus applied electric field (P-E) for pure BFO₃ and La 3% doping in BFO₃ samples at low frequency of 50 Hz at room temperature. With the increase of applied electric field, the polarization increased and showed saturation. The

remnant polarization shows decreasing with the increase of La dopant concentration, in contrast with the coercivity, which exhibit an increase in sequence with the increase of La content.

REFERENCES

- [1]. Fiebig, M. 2005. Revival of the magnetoelectric effect. *J. Phys. D: Appl. Phys.* 38: R123-R152.
- [2]. Hill, N, A. 2000. Why are there so a few magnetic ferroelectrics? *J. Phys. Chem. B*, 104: 6694–6709.
- [3]. Chaudhuri, A. K, Mandal. 2012. Enhancement of ferromagnetic and dielectric properties of lanthanum doped bismuth ferrite nanostructures. *Materials Research Bulletin* 47(4):1057–1061.
- [4]. X, Chen. H, Zhang. K, Ruan. W, Shi. 2012. Annealing effect on the bipolar resistive switching behaviors of BiFeO₃ thin films on LaNiO₃-buffered Si substrates, *J. Alloy. Compd.*, 529: 108–112.
- [5]. Lazenka, V, V. Ravinski, A, F, Makoed. Vanacken I, I. Zhang J. G., Moshchalko, V, V. 2012. Weak ferromagnetism in La-doped BiFeO₃ multiferroic thin films. *J. Appl. Phys.*, 111, 123916,
- [6]. Yuan, G, L. Or S, W., Liu J. M., Liu Z. G. 2006. Structural transformation and ferroelectromagnetic behavior in single-phase Bi_{1-x}Nd_xFeO₃ multiferroic ceramics. *Appl. Phys. Lett.* 89, 052905
- [7]. Li, J. Duan, He, Y, H. Song, D. 2001. Crystal structure, electronic structure, and magnetic properties of bismuth-strontium ferrites. *J. Alloys Compd.* 315: 259–264.
- [8]. M. A. Ahmed, E. Dhahri, El-Dek, S. I. and Ayoub, M. S. 2013. Size confinement and magnetization improvement by La³⁺ doping in BiFeO₃ quantum dots, *Solid State Sci.*, 20: 23–28.

- [9]. T. Ahmed, A. Vorobiev, S. Gevorgian, 2012. Growth temperature dependent dielectric properties of BiFeO₃ thin films deposited on silica glass substrates. *Thin Solid Films*, 520: 4470–4474.
- [10]. Casper M, D. Losego, M, D. Maria, J, P. 2013. Optimizing phase and microstructure of chemical solution-deposited bismuth ferrite (BiFeO₃) thin films to reduce DC leakage. *J. Mater. Sci.*, 48: 1578–1584.
- [11]. Maxwell, J, C. 1873. Electricity and Magnetism, Oxford University Press, vol. 1 pp. 328.
- [12]. Prodromakis, T. Papavassiliou, C. 2009. Engineering the Maxwell–Wagner polarization effect. *Appl. Surf. Sci.* 255: 6989-6994
- [13]. Koop, C. 1951. On the Dispersion of Resistivity and Dielectric Constant of Some Semiconductors at Audio frequencies. *Phys. Rev B*. 83:121